The beginning of a dark matter adventure

Bachelor thesis

Angela Büchler

January 12, 2006

Abstract

Baseline of this work is the development of a liquid argon detector for dark matter particles. From astrophysical research one supposes, that cold dark matter is distributed in a halo around galaxy centres, modifying the gravitational potential, derived from the observed visible matter.

Elementary particles, so called WIMPS (Weakly Interacting Massive Particles) are widely believed to be a plausible solution for the dark matter puzzle. The neutralino, the lightest super symmetrical particle, seems to be therefore the hottest candidate, being only subject to weak and gravitational interaction. In a collision of a WIMP with an Ar-Atom, the recoiling nucleus produces free charges as well as scintillation light in the vacuum-UV (128 nm).

This bachelor thesis concerns the first development of the light detection system for such a detector. Therefore a 5 liter prototype was built, which could be filled with gaseous or liquid argon. An α-source placed inside served for the excitation of the argon atoms, while the light was read out with wavelength shifting material and a phototube. To investigate the scintillation mechanism of argon and in particular the overall light yield of the readout system, large emphasis was put to reconstruct precisely the number of measured photoelectrons from the photomultiplier signals. This was also done under variation of the contamination of gaseous argon with air. The readout system allowed for a determination of the time response of UV light emission in gaseous argon. Both, the light emission from the singlet (fast) and triplet (slow) excited molecular states of argon, could clearly be identified by their characteristic decay times. This yields the first step towards the capability of a liquid argon detector, to discriminate among different particles which, interacting with argon, modify the population of the produced singlet and triplet states. The ionisation density dependent population of the singlet and triplet states in liquid argon is projected to be used for an identification of interacting particles and hence one of the key parameters in the development of such a detector.

Contents

List of Tables

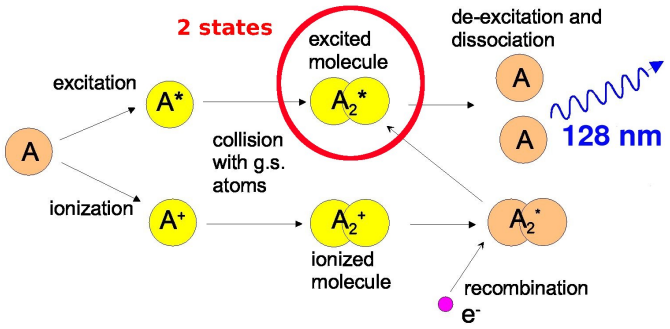

Figure 1: Production scheme for 128 nm light in argon [1].

1 Scintillation mechanism in argon

Ionizing particles impinging on dense noble gases such as argon or xenon, initially produce excited, as well as ionized gas atoms (see Fig. 1). Under the interaction with neutral gas atoms, in the case of argon, excited A_2^* molecules are finally produced in two different states, namely a triplet $^3\Sigma_u^+$ and a singlet $^1\Sigma_u^+$ molecular state. Both of these decay radiatively with different time constants, in a narrow band around 128 nm. This light is not absorbed from individual gas atoms, causing hence the good scintillation behaviour of noble gases. For a more detailed description the reader is referred to references [2,3] and citations therein. Since different particle interactions, e.g. by fission fragments, electrons or neutrons produce different ionization densities and hence different populations of the singlet and triplet states [2], the structure of the scintillation light can be used to discriminate among the particle types. This will be one of the key features of a future liquid argon dark matter particle detector to be developed and it goes in hand with a good light yield of the 128 nm detection system.

2 Experimental setup

A cylindrical vessel forms the main part of the setup (see Fig. 2). For the measurements it was pumped and filled with air or argon. The pump system consists of a dry primary pump and a turbo pump, reaching around 10^{-6} mbar final pressure at room temperature in the vessel. To the right, a quadrupole mass spectrometer (QMS) is connected. Different tubes connect the gaseous argon bottle (class ^{60}Ar; impurities $\leq$ 1.3ppm [4]) and the liquid argon tank to the vessel. Several pressure gauges are mounted for controlling the vacuum (Fig. 3). Fig. 4 and Fig. 5 show the interior of the vessel. The photomultiplier (Hamamatsu R580, 38 mm diameter, 10-stage, bi-alkali photo cathode [5]) is located at the centre of the setup, wearing a

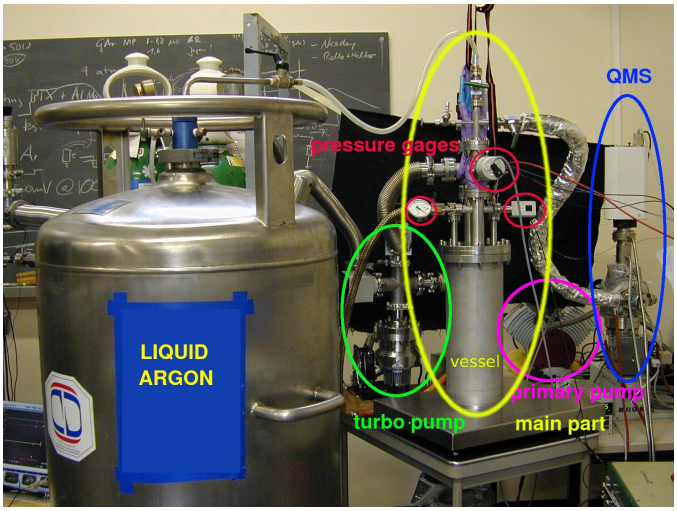

Figure 2: Laboratory setup.

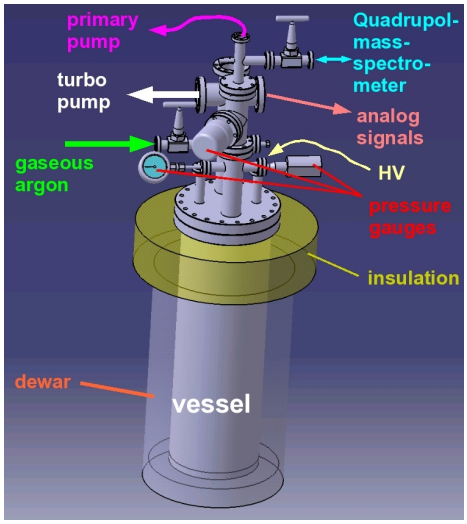

Figure 3: Technical drawing of the vessel with the different connectors of the pumping, the gaseous argon bottle, the QMS, the signal outlet etc.

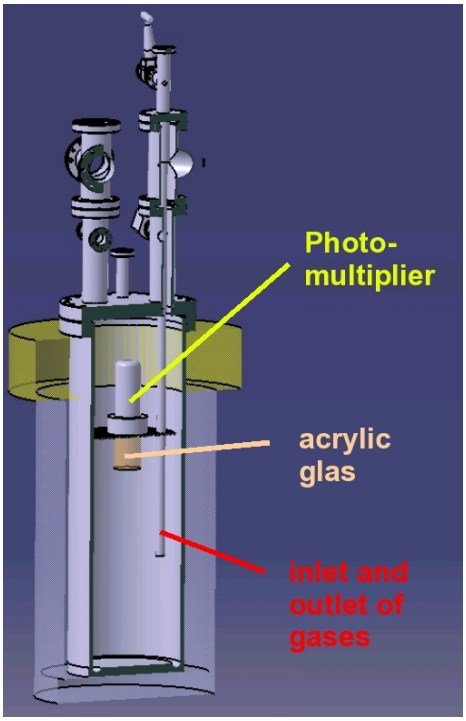

Figure 4: Inside of the vessel, inlet/outlet tube, photomultiplier pointing downwards shielded with acrylic glass.

Figure 5: Inside the vessel. The geometry used for the measurements with the phototube, pointing downwards.

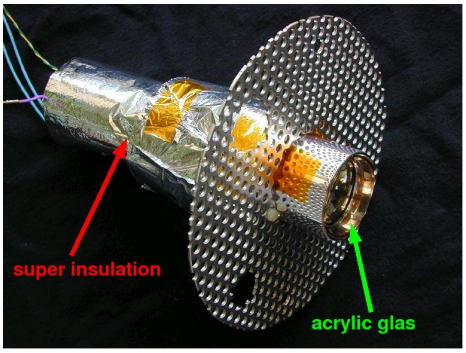

Figure 6: Photomultiplier prepared for measurements with liquid argon. The low temperature protection (super insulation and acrylic glass light guide) can be seen.

highly reflecting [1] collar (MgF_2 coated aluminium reflector). On its side, a special tube serves as intake and outlet for argon or air. About 6 cm below the photomultiplier a ^{210}Po α-source (30 Bq, 5.3 MeV) was installed, to excite the argon atoms with a light yield of 67.9 eV/UV photon [1]. 78′000 photons (128 nm) are created by the emission of one α-particle, if the argon is very pure. Fig. 6 shows the photomultiplier prepared for measurements with liquid argon, which are not described in this report. To protect the photomultiplier against the low temperature a heating and super insulation was introduced, as well as a cylindrical acrylic glass spacer. Then several methods were invented to measure the liquid level in the vessel. A platinum temperature sensor, a floater and a balance gave informations about the filling level. The vessel itself was surrounded by liquid argon in a dewar to ensure cooling.

2.1 Enhancing performance with a wavelength shifter

Due to the relatively high cut off to short wavelength (Fig. 7) of the photomultiplier, a wavelength shifter had to be introduced into the system. A tetratex-teflon foil (250 μm thick) was coated with TPB (tetra-phenyl-butadien) and attached on the inside walls of the vacuum vessel. The TPB, emitting at 420 nm, was dissolved in chloroform and sprayed with different vaporizers onto the tetratex foil. The chloroform evaporated in short time, leaving behind a thin film of TPB. By illumination of the tetratex samples with a 250 nm UV lamp (Fig. 8), the wavelength shifting behavior of the

[1] for wavelengths down to 120 nm

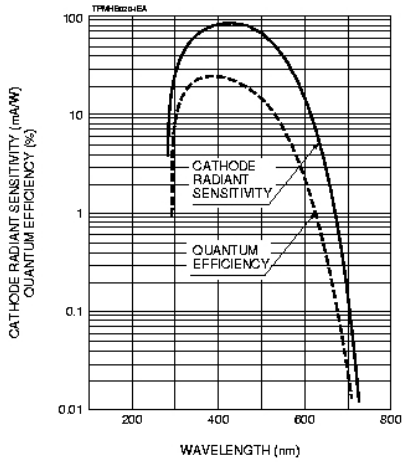

Figure 7: Sensitivity and quantum efficiency of the photomultiplier [5].

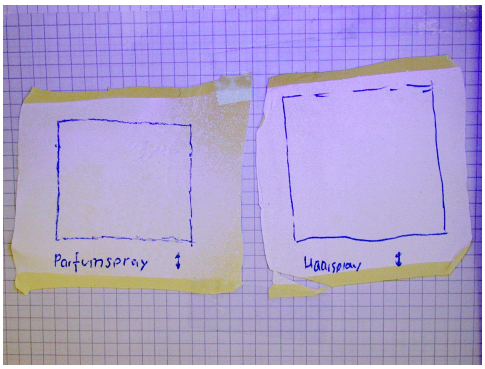

Figure 8: Tetratex with TPB, sprayed with different vaporizers, shining in the blue.

TPB was tested. Also note the yellowish reflecting borders, onto which the TPB was not sprayed. Tetratex as base material was chosen for its good properties for diffusely reflecting light, yielding a rather homogeneous light collection in the setup by geometrically different light sources. Due to the teflon nature of the tetratex foil, the setup withstood easily liquid argon temperatures ($-200°$C).

3 Measurements

3.1 Data reconstruction

The Hamamatsu photomultiplier (type R580) was operated with $-1'350$ V bias voltage yielding roughly a gain of 10^6. Its signal was amplified by a factor of 10 in a fast NIM amplifier and fed to the 8 bit FADC at a LeCroy WP7'100 oscilloscope, terminated with 50 Ω (Fig. 9). The 8 bit resolution can be observed in Fig. 11 (see below). Data was taken with the settings of 1 GS/s and $20'002$ data points per event, covering 20 μs of readout time. The data was written to the hard disk of the oscilloscope in compressed MatLab file format in packages of $2'000$ to $5'000$ events. The event trigger in the oscilloscope was set on the analog signal height in the range of -20 to $-2'000$ mV, depending on the data set to be taken. The typical height of a single photo electron pulse after the 10x amplification amounted to roughly -35 mV. The raw data files were further on analyzed with MatLab off line. Fig. 10 shows a typical α-event in gaseous argon plotted from data taken at $1'200$ mbar at a partial air pressure of 10^{-6} mbar. To reconstruct the total

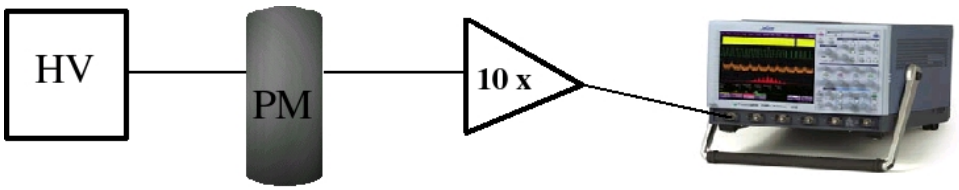

Figure 9: Data reconstruction: the photomultiplier (PM) runs with high voltage (HV), the signal is amplified 10x and channelled to the oscilloscope.

number of measured photoelectrons, the integrated signal (=pulse height) was divided by the averaged integrated signal of single photo electron events. Before numerical integration (in MatLab, function cumsum) the pedestal was determined event-wise by averaging over the first couple of thousand data points before the trigger [2] and subtracted from the raw signal. The pulse height was then determined by averaging over the last 5′000 data points of the integrated signal (Fig. 18). This value was later on histogrammed (see Fig. 13, 14, 15). The peak from α-particles is clearly visible in all data sets and colored in red. Mean μ, standard deviation σ and error of the mean m_μ were determined from these events with the MatLab function centroid. The number of photoelectrons was derived by dividing μ by the calibration factor described in the next chapter.

3.2 Calibration

The purpose of the calibration was the most precise determination of the single photon pulse height and hence the total number of observed photoelectrons in an event. Two different methods were investigated: dark count measurement and extraction of the single photon pulse height from the event tails. The former was later on chosen due to higher statistics and due to a discovered correlation of the single photon pulse height to the total pulse height (pile-up) in the second method.

3.2.1 Extraction of the single photon pulse height from the data

A typical signal from an α-event can be seen in Fig. 10. The red circle shows the small peaks from late arriving photons after the event. All peaks with amplitudes smaller than a threshold of -0.0065 V were selected, and for correct integration, five data points to the left and the right of the peak were added. As in the previous chapter, the pulse height was calculated and histogrammed. The average single photon pulse height was determined as the mean of the histogram. The results from different data sets are displayed

[2] accidental signal entries were disregarded by a threshold of -20 mV

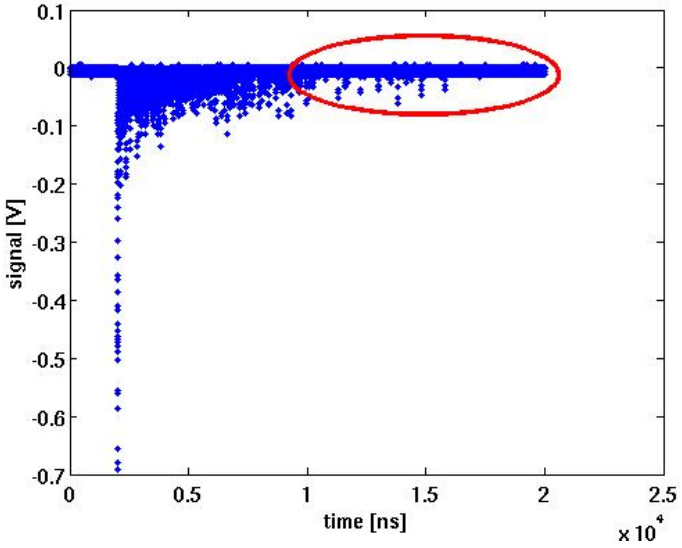

Figure 10: Typical α-event in gaseous argon, the red circle marks the region taken for the calibration.

in table 1. They show the above mentioned correlation of the average single photon pulse height with the total signal height in the events.

Table 1: Calibration extracted from data, for different purity of argon

$single\,photon\,height\,[V \cdot ns]$	$entries$	$\mu\,(mean\,of\,the\,\alpha peak)$
0.15565	700	87.8496
0.15141	700	85.8449
0.15634	700	82.4465
0.15562	700	80.1130
0.15076	700	64.8910
0.16182	700	106.2107
0.16229	700	106.9064
0.15899	700	103.3214

3.2.2 Dark count measurement

To determine the spectrum of thermally ejected electrons from the photocathode the photomultiplier was in the dark in a good vacuum (10^{-5}mbar) in order not to generate scintillation light from gas atoms. Thermally emitted electrons generate the same signal height as electrons emitted by photo-effect

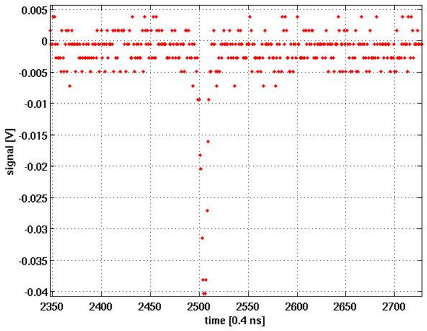

Figure 11: Typical dark count event, the 8 bit resolution of the scopes FADC can clearly be seen.

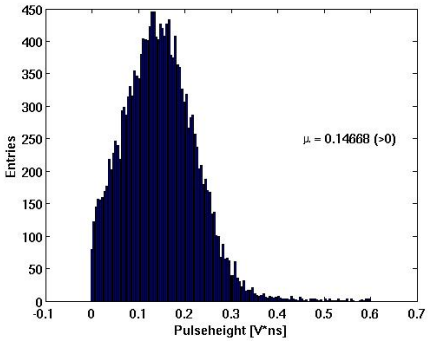

Figure 12: Histogram of 18'000 integrated dark count entries.

from the photo-cathode. These signals were recorded. A typical signal is shown in Fig. 11. Integration and histogramming of the peaks gave the single photon pulse height distribution (Fig. 12). From this histogram the mean value μ was determined by the centroid function:

$$\mu = \frac{s * binc}{sum} \tag{1}$$

where s is the bincontent of the single photon pulse height distribution, binc the bin center and sum the sum of single photon heights.

The average single photon pulse height was found to be 0.1467 ± 0.005 V, with $18'000$ entries (Fig. 12). The error on μ was estimated by comparing to the first method for the calibration, the extracted single photon pulse height from the data, so a systematical error is included. Any further calculations are based on this value.

3.3 Number of photoelectrons in argon gas

3.3.1 First measurements with TPB only at the bottom

After determination of the single photon line in vacuum (which was repeated from time to time to confirm the calibration) the vessel was filled with clean argon gas up to a pressure of typically $1'100$ mbar. In a first test only the bottom of the vessel (ca. 150 cm^2) was covered by TPB coated tetratex. The pulse height distribution (as described in chapter 3.1) from α-particles is shown in Fig. 13. The peak colored in red is attributed to the interaction of α-particles with the argon gas. Table 2 shows the results of a series of 3 measurements, leading to roughly 50 photoelectrons per event. The error

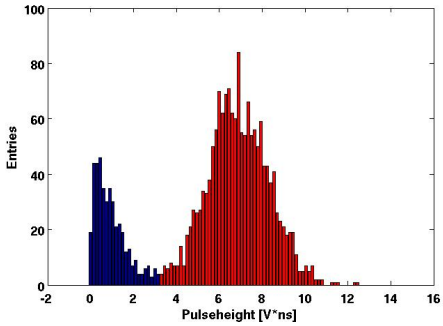

Figure 13: First measurement with TPB only at the bottom, 47 photoelectrons, 2′023 entries.

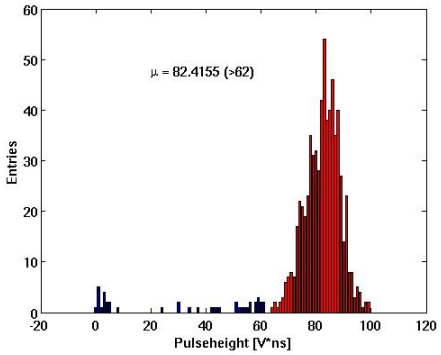

Figure 14: Pulse height distribution with complete TPB coverage corresponding to 562 photoelectrons for 700 entries.

Table 2: First measurements with TPB only at the bottom

photoelectrons	*entries*	*comment*
47.0176 ± 1.6210	2′023	Fig. 13, page 10
58.3743 ± 2.0797	1′002	
50.5251 ± 1.8239	1′001	

m_μ of the mean pulse height was estimated as follows:

$$m_\mu = \frac{\sigma}{\sqrt{N}} \tag{2}$$

where $\sigma =$ is the standard deviation (see 3.1), and N the number of entries. The error on the number of photoelectrons was then calculated with the common error propagation laws. This light yield is very low when compared to the nominal value of 78'000 produced photons per α-particle in gaseous argon.

3.3.2 Complete TPB coverage

The apparatus was opened and the walls and all tubes inside the vessel were covered with the wavelength shifting material TPB on the surface of the tetratex. The bottom was resprayed with TPB. Fig. 14 and table 3 show the results of the measurements. A drastic increase in light yield (from 50 to 500 p.e. roughly) and a strong dependence on the cleanness of the argon gas was found. This effect is discussed in more details in the next section.

Table 3: Complete TPB coverage (see also Fig. 14)

$Numberofphotoelectrons$	$entries$
598.9 ± 20.6	700
585.6 ± 20.1	700
561.9 ± 19.2	700
545.7 ± 18.7	700
442.0 ± 15.2	700

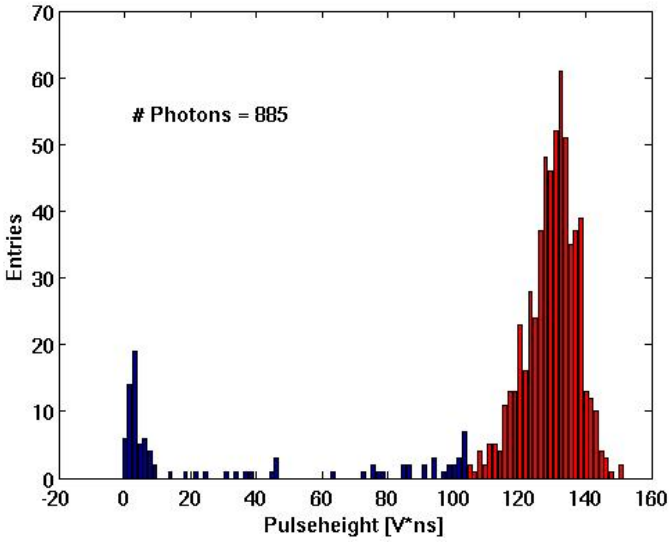

Figure 15: Pulse height distribution of absorption measurement, 700 entries.

3.4 Light yield as a function of purity of the argon gas

The purpose of these measurement was to find out the influence of air contamination on the light yield of argon. The cleanness depended mostly on the vacuum pressure in the vessel before letting argon in. At a low pressure, more photoelectrons were detected, because the amount of residual oxygen and water was smaller. An interesting question was, whether a lower limit of pressure existed, for which the number of photoelectrons did not increase significantly anymore. Different measurement sequences were tried out:

Sequence 1: the argon was pumped out to a pressure of $3 \cdot 10^{-3}$ mbar and the pumps were closed. Air was then let in up to atmospheric pressure, then pumped out until the desired vacuum was reached. Finally gaseous argon was let in up to $1'100$ mbar and the high voltage was

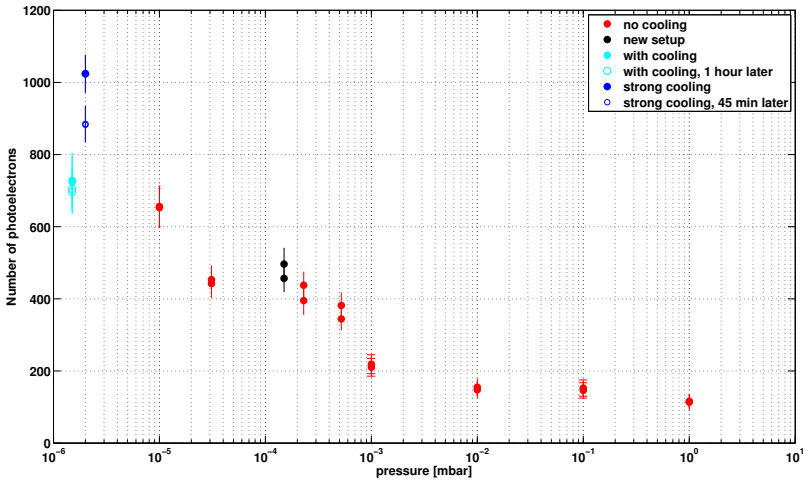

Figure 16: Semilogplot number of photoelectrons (table 4), showing clearly the dependence on the purity of the argon.

switched on for data taking.

Sequence 2: the argon was pumped out to $3 \cdot 10^{-3}$ mbar and the pumps were closed. Air was let in up to the desired pressure. Then the volume was filled with argon to a pressure of $1'100$ mbar. High voltage was switched on and data were taken.

As tests showed, sequence 1 provided better and more reproducible results and the pressure was also easier to be controlled. Fig. 16 shows in a semilogplot the number of photoelectrons for the data of table 4. The number of p.e. was calculated as in the previous chapter (eq. 2). The error of the mean pulse height m_μ was estimated as usual as well as the error of the number of photoelectrons.

3.4.1 Discussion of the results

The number of photoelectrons clearly depends on the purity of the argon. For each sequence, two batches of data were taken consecutively, the second about $10 - 15$ min later than the first (for technical reasons). As table 4 shows, the number of photoelectrons decreased after $10-15$ min between the first and the second data taking (when the vessel was not cooled). The outgassing of the tetratex is assumed to be responsible for this effect, over all due to H_2O (this was confirmed with the quadrupole mass spectrometer). On the contrary, with continuous cooling, the second batch contained slightly more photoelectrons. We assume, that here the water molecules were freezing out.

Table 4: Light yield measurement, for 700 entries each. Two batches of data were taken of each pressure, separated by $10 - 15$ min.

$p\,[mbar]$	$No\,of\,p.e.$	*comments*
1	116.0 ± 18.7	no cooling
1	113.4 ± 20.1	no cooling
10^{-1}	152.5 ± 22.5	no cooling
10^{-1}	146.1 ± 21.2	no cooling
10^{-2}	154.9 ± 22.6	no cooling
10^{-2}	147.8 ± 21.7	no cooling
10^{-3}	218.6 ± 26.2	no cooling
10^{-3}	210.2 ± 24.7	no cooling
$5.2 \cdot 10^{-4}$	381.6 ± 35.5	no cooling
$5.2 \cdot 10^{-4}$	344.2 ± 30.6	no cooling
$2.3 \cdot 10^{-4}$	437.6 ± 36.1	no cooling
$2.3 \cdot 10^{-4}$	395.1 ± 37.9	no cooling
$1.5 \cdot 10^{-4}$	496.3 ± 43.7	new setup
$1.5 \cdot 10^{-4}$	456.7 ± 36.2	new setup
$3.1 \cdot 10^{-5}$	453.1 ± 38.3	no cooling
$3.1 \cdot 10^{-5}$	442.3 ± 39.3	no cooling
10^{-5}	656.0 ± 56.8	no cooling
10^{-5}	652.6 ± 53.3	no cooling
$2 \cdot 10^{-6}$	1023.8 ± 69.8	strong cooling
$2 \cdot 10^{-6}$	1024.0 ± 74.3	strong cooling
$2 \cdot 10^{-6}$	882.5 ± 61.2	strong cooling, 45 min later
$2 \cdot 10^{-6}$	885.0 ± 60.7	strong cooling, 45 min later
$1.5 \cdot 10^{-6}$	723.8 ± 51.2	with cooling
$1.5 \cdot 10^{-6}$	728.5 ± 49.9	with cooling
$1.5 \cdot 10^{-6}$	704.4 ± 46.7	with cooling, 1 h later
$1.5 \cdot 10^{-6}$	696.4 ± 48.9	with cooling, 1 h later

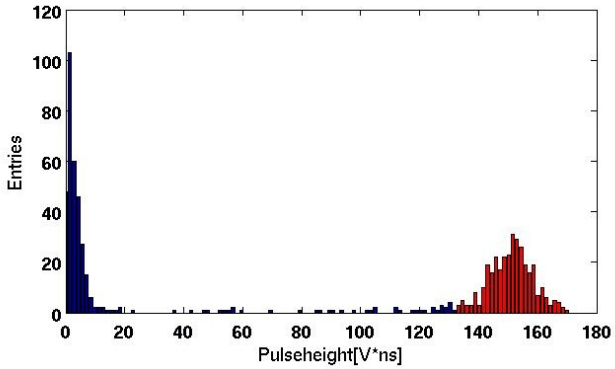

Figure 17: Pulse height distribution with the 332 good α-events marked in red.

Furthermore, the lower limit of pressure, for which the number of photoelectrons was not increasing significantly could not be found. Fig. 16 illustrates, that the number of photoelectrons still rises below pressures of 10^{-5} mbar [3]. There is an uncertainty in the pressure value for the cooled data, because the partial pressures of argon, water and oxygen were not studied in detail at low temperatures.

An α-particle of 5.3 MeV produces 78′000 photons. With 1′023 photoelectrons for the best light yields and with a quantum efficiency of the phototube of max 20%, around 5′115 photons entered the phototube. Therefore we conclude: the remaining photons were not seen either due to absorption of the 128 nm light, inefficient conversion of the wavelength shifting material or bad light collection [4]. The fraction of collected photons then amounts to 6.6%. This is already a promising number for the development of a detector working with these very short and highly ionising wavelength of vacuum ultraviolet (VUV) radiation (128 nm).

3.5 Time structure of α-events in gaseous argon

The data sample with the mean of 1′023 photoelectrons at $2 \cdot 10^{-6}$ mbar, was chosen for analysing the time structure of the α-events in gaseous argon. The signal amplitude of the 700 entries was integrated numerically as described in chapter 3.1 and histogrammed. α-events were selected by eye via 2 cuts at 130 and 170 Vns (red events in Fig. 17, 332 out of 700). The average of

[3] 10^{-6} mbar was unfortunately the limited vacuum pressure which could be achieved with the pump system.

[4] A further analysis of the data, which is not described in this report, showed absorption of VUV photons in the argon-air mixture being negligible for partial pressures of air below 10^{-2}mbar.

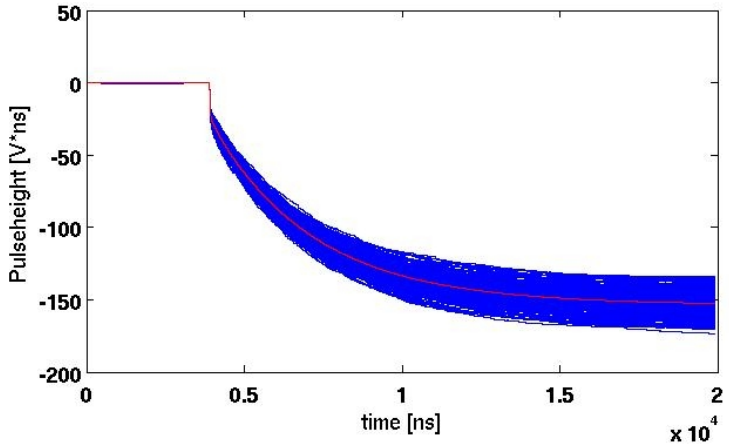

Figure 18: Integrated signal amplitude as a function of time of these selected 332 events (blue) and their average (red).

their integrated signal amplitudes (Fig. 18) was used further on for the time structure analysis after numerical differentiation (MatLab function diff).

This signal amplitude as a function of time (Fig. 19) was fitted by a function with 6 parameters and the χ^2 method. The function was built as a convolution of a Gaussian with a step function, multiplied with two exponential decays. The exponential decays correspond to the decay of the singlet and triplet molecular states:

$$fitfunction = gauss(t,\sigma) * step(t-t_0) \cdot \left(\frac{A}{\tau_1} \cdot e^{-\frac{t-t_0}{\tau_1}} + \frac{B}{\tau_2} \cdot e^{-\frac{t-t_0}{\tau_2}} \right) \quad (3)$$

with

$$step(t-t_0) = \begin{cases} 0 & \text{for } t < t_0 \\ 1 & \text{for } t > t_0 \end{cases} \quad (t_0 > 0) \quad (4)$$

and where

$\boldsymbol{t_0}$ corresponds to the event time,

$\boldsymbol{\sigma}$ of the Gaussian represents the experimental time resolution,

$\boldsymbol{A}, \boldsymbol{B}$ [nVs] correspond to the numbers of photoelectrons of the fast and slow components respectively,

$\boldsymbol{\tau_1}, \boldsymbol{\tau_2}$ are the decay-times of the fast and slow components respectively.

The fit is in good agreement with data. Both decays from the two states are clearly visible. The fitted radiative lifetime τ_2 for the triplet state (slow component) also agrees with a published value 3.2 ± 0.3 μs [3]. The decays occur with a ratio of $\frac{853}{143} \sim \frac{5.3}{1}$ (triplet to singlet components).

population singlet state	=	143 ± 17
population triplet state	=	853 ± 13
$\boldsymbol{\tau_1}$	=	15.7 ± 4 ns
$\boldsymbol{\tau_2}$	=	$3'120 \pm 80$ ns

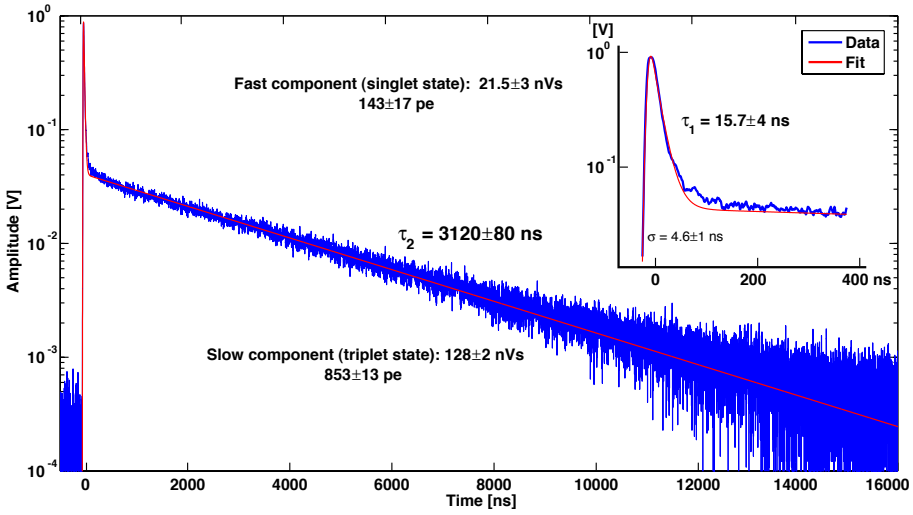

Figure 19: Reconstructed signal amplitude as a function of time including the fit. Fast (small inset to the right) and slow components of the decays of the two molecular states are visible.

4 Summary

A vacuum chamber was built which can be filled with gaseous and liquid argon. A maximum light yield of roughly 7% was acchieved, which is a promising number for VUV light detection. The effect of air contamination of the argon was measured. H_20 is thereby the dominating impurity. Two components in the decay time structure of scintillation light could clearly be identified, they correspond to the singlet and triplet molecular states of argon. The population of the singlet and triplet states, depending on the ionization density, is an important observable for a future liquid argon dark matter detector (background suppression).

5 Acknowledgements

Special thanks go to Claude Amsler, who gave the opportunity for joining his group at the CERN laboratory for this bachelor thesis and for overseeing the process of my work as well as for final corrections. Many thanks for the great technical support during the two months go to Christian Regenfus and Jacky Rochet, making the experiment a success. Thanks to Jacky Rochet who produced the technical drawings. My best thanks go to Christian Regenfus as well for the coaching and his large supporting advise on writing my first thesis.

References

[1] R. Chandrasekharan, M. Messina, A. Rubbia, *Detection of noble gas scintillation light with large area avalanche photodiodes (LAAPDs)*, Nuclear Instruments and Methods in Phys. Res. A546(2005)426

[2] A.Hitachi et al., *Effect of ionization density on the time dependence of luminescence from liquid argon and xenon*, Phys. Rev. B27(1983)5279

[3] J. W. Keto et al., *Production Mechanisms and Radiative Lifetimes of Argon and Xenon Molecules Emitting in the Ultraviolet*, Phys. Rev. Letters 33(1974)1365

[4] alphagaz product table: *http://www.carbagas.ch/GasCat_f/alphagaz.htm*, (11. Jan. 2006)

[5] Hamamatsu, *Specifications Photomultipliertube R580*, Japan, December 1999